Materials Transactions, JIM, Vol. 34, No. 10 (1993), pp. 919 to 929

Mechanism of the A_s Temperature Increase by Pre-deformation in Thermoelastic Alloys

Min Piao*†, Kazuhiro Otsuka*, Shuichi Miyazaki*
and Hiroshi Horikawa**

*Institute of Materials Science, University of Tsukuba, Tsukuba, Ibaraki 305, Japan
**Yokohama Laboratory, Furukawa Electric Co. Ltd., Yokohama 220, Japan

The Ti-Ni-Nb shape memory alloys are attracting recent attention for the wide transformation temperature hysteresis, which is caused by the A_s increase due to pre-deformation, since it is suitable for pipe couplings. To find out the origin for the A_s increase by pre-deformation, similar investigation was made by tensile tests, electrical resistance measurements, optical microscopy and transmission electron microscopy (TEM), for a Cu-13.8%Al-4.0%Ni (mass%) single crystal, and Ti-50%Ni and Ti-50.5%Ni (at%) polycrystals, which exhibit the thermoelastic martensitic transformation. The increase of A_s due to pre-deformation was confirmed in these alloys as well. When the single crystal was elongated to the end of the first stage of the stress-strain curve in the martensitic state, which corresponds to the rearrangement of martensite variants without permanent strain, A_s increased. On the other hand, the A_s increase in polycrystals was found to be closely related with the introduction of the permanent strain. Furthermore, the effect of pre-deformation was found to be erased by the subsequent reverse transformation, as is reported for Ti-Ni-Nb alloys. For that effect, we propose a mechanism, by focusing attention on the elastic strain energy stored during the thermoelastic martensitic transformation, which can explain the observed effect well.

(Received June 14, 1993)

Keywords: *thermoelastic alloy, thermoelastic martensitic transformation, martensitic transformation, hysteresis; shape memory alloy, titanium-nickel, nickel-titanium, titanium-nickel-niobium, copper-aluminum-nickel, pipe coupling*

I. Introduction

Ti-Ni-Nb ternary shape memory alloys have attracted considerable attention in recent years, since they exhibit a wide transformation temperature hysteresis upon suitable mechanical treatment, which is quite useful for the applications for coupling and sealing[1][2]. The changes of the microstructure and the transformation temperature of Ti-Ni-Nb alloys as a function of composition[3] and the mechanical behavior of the $Ti_{44}Ni_{47}Nb_9$ alloy[4] were investigated rather systematically by the present authors recently.

In the Ti-Ni-Nb alloys with proper compositions, A_s (reverse transformation start temperature) is raised remarkably by pre-deformation in the martensitic or stress-induced transformation temperature range (compared to the original A_s), thus increasing the transformation temperature hysteresis of the alloy. This effect was first found by Melton *et al.*[1][2], and studied more in detail by Zhao *et al.*[5]-[7] and the present authors[4]. The characteristic of this effect may be summarized as follows. A_s increases with increasing amount of pre-deformation. After the first reverse transformation, A_s turns back to a lower temperature, which is close to the original A_s, and becomes constant in the following thermal cycles. By electron microscopy work, Zhao *et al.*[5] found that the alloy after solution-treatment consists of the Ti-Ni phase (containing a small amount of Nb), which is responsible for the shape memory effect (SME), and the Nb-rich phase (bcc), which does not transform. Duerig *et al.*[8][9] ascribed the above effect to the presence of the Nb-rich phase, and explained the effect in the following way. If a Ti-Ni-Nb alloy is deformed, the Ti-Ni matrix deforms reversibly by the usual twin boundary motion, while the Nb-rich phase deforms irreversibly via slip. Upon heating, the matrix tries to recover its original shape, but the Nb-rich phase resists the shape recovery process effectively providing a frictional stress. Thus, the irreversible deformation of the Nb-rich phase delays the recovery, increasing A_s. Meanwhile, there is a report[10] that the reverse transformation temperatures increase by deformation in a Ti-Ni binary alloy, although it is very brief. Thus, the above effect may be common in other alloys as well. If that is the case, Duerig *et al.*'s mechanism does not apply to these cases, where no Nb-rich phase is present.

The purpose of the present work is thus two-fold. The first is to investigate the effect of pre-deformation on the reverse transformation of thermoelastic alloys such as Cu-Al-Ni and Ti-Ni alloys. The second is to look for the origin for the increase of A_s by pre-deformation.

As a possible such origin, we focus attention on the elastic strain energy stored during the thermoelastic martensitic transformation. The effect of such elastic energy was already discussed by Tong and Wayman[11],

† Graduate Student, University of Tsukuba.

and the effect was mathematically formulated by Olson and Cohen[12]. Following the latter, the thermodynamic equilibrium for a martensite plate and the parent phase is described by the following equation:

$$\Delta g_{ch}+2\Delta g_{el}=0,$$

where $\Delta g_{ch}=g_M-g_P$ is the chemical free energy change between parent and martensite, and Δg_{el}, is the elastic strain energy stored around the martensite plate. The above equation means that the half of the chemical free energy change is stored as the elastic energy in the specimen. This elastic energy is expected to resist the forward transformation, and to assist the reverse transformation, and the presence of such effect was observed in the comparison of single interface vs. multiple interface transformations upon cooling and heating[13].

II. Experimental Procedure

The materials used in this study were the single crystal of Cu-13.8%Al-4.0%Ni (mass%) alloy and the polycrystals of Ti-50%Ni, Ti-50.5%Ni and Ti-47%Ni-9%Nb (at%) alloys. They are represented by Cu-13.8Al-4.0Ni, $Ti_{50}Ni_{50}$, $Ti_{49.5}Ni_{50.5}$ and $Ti_{44}Ni_{47}Nb_9$ respectively.

The single crystal of Cu-13.8Al-4.0Ni alloy was made by the Bridgman method, and the orientation was determined by the back reflection Laue method. Specimens for tensile tests and electrical resistance measurements were spark-cut into $50\times1.5\times1.5$ (mm^3) size along $\langle001\rangle_{\beta1}$ orientation. The specimens were annealed for 3.6 ks in a vacuum of 10^{-3} Pa at 1273 K, followed by quenching into ice water, and then annealed at 523 K for 3.6 ks. The latter heat-treatment at 523 K was necessary to insure that the martensite is a γ_1' single phase[14]. After the heat-treatments, the specimens were mechanically polished with emery papers at a temperature in the parent state, and electropolished in the supersaturated phosphoric acid-chromium oxide (CrO_3) solution in the parent state. Tensile tests were carried out with an Instron type machine, Shimadzu Auto-graph DDS-10T-S. Electrical resistance measurements were made with heating→cooling→heating cycle, to observe the characteristics of the martensitic transformation and to determine the transformation temperatures. The effect of deformation on the transformation was investigated by measuring the electrical resistance after tensile test. Observations for martensite variants and their rearrangement process with deformation were performed by using optical microscope with polarized light.

The Ti-Ni and Ti-Ni-Nb alloys were melted in a high frequency vacuum furnace, and the ingots were hot-worked and cold-rolled into strips with approximately 0.7 mm thickness. Specimens for tensile tests and electrical resistance measurements were spark-cut into $50\times1.4\times0.7$ (mm^3). They were annealed for 3.6 ks in a vacuum of 10^{-3} Pa at 1173 K, followed by quenching into ice water. These specimens were mechanically polished with emery papers first, and then electropolished in $HClO_4$(60%):$(CH_3CO)_2$=7.5:92.5(vol.) solution at 283 K for $Ti_{50}Ni_{50}$ and $Ti_{49.5}Ni_{50.5}$ alloys while in H_2SO_4:CH_3OH=15:85(vol.) solution at 243 K for $Ti_{44}Ni_{47}Nb_9$ alloy. Tensile tests and electrical resistance measurements were carried out by the same method as that for the Cu-13.8Al-4.0Ni alloy. JEM-200CX transmission electron microscope (TEM) was used at 200 kV for observing martensite variants and internal structures, since the variants in these alloys are so small that they can not be observed with optical microscope. Samples for TEM observation were prepared as follows. Tensile specimens with $40\times4.0\times0.5$ (mm^3) gauge portion were prepared by the method as mentioned above. They were tensile tested to various total strains, and then chemically thinned to about 0.12 mm thickness by immersing them in HF:HNO_3:H_2O=1:4:5(vol.) solution. Discs of 3 mm diameter were spark-cut from the gauge portion of each specimen. The discs were mechanically polished on 1000-1500 grit emery papers with the best of care, and jet-electropolished into TEM samples. The solutions used in the jet-electropolishing were the same as the electropolishing solutions. The observations were performed at room temperature and at 523 K by using a heating holder.

III. Results

1. Increase of the A_s temperature in a Cu-Al-Ni single crystal

We first discuss the simplest case of a Cu-Al-Ni single crystal. The transformation temperatures of the alloy determined by electrical resistance measurement were: M_s=341 K, M_f=334 K, A_s=362 K and A_f=387 K. Thus the specimen was in a martensitic state at room temperature. Figure 1 shows a stress-strain (abbreviated below as S-S) curve of the alloy single crystal at room temperature. We observe a clear first stage on a very low stress level with a strain up to 6%. As will be evidenced soon, this stage corresponds to the reorientation of the martensite variants. We confirmed that the strain in this stage recovered completely without any permanent strain after heating to a temperature above A_f. Figure 2(a)-(e) are optical micrographs corresponding to the first stage Fig. 1. Figure 2(a) shows a typical γ_1' (orthorhombic) martens-

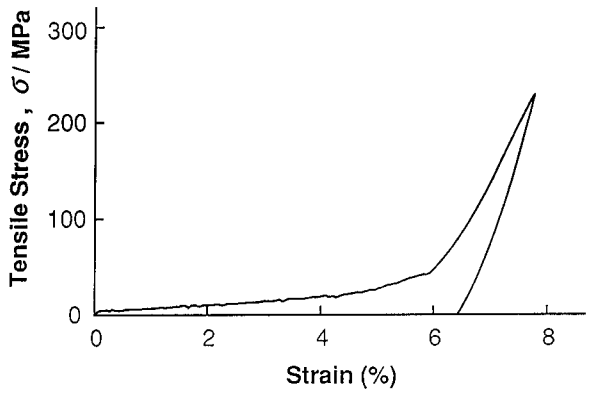

Fig. 1 Stress-strain curve of a Cu-13.8Al-4.0Ni alloy single crystal.

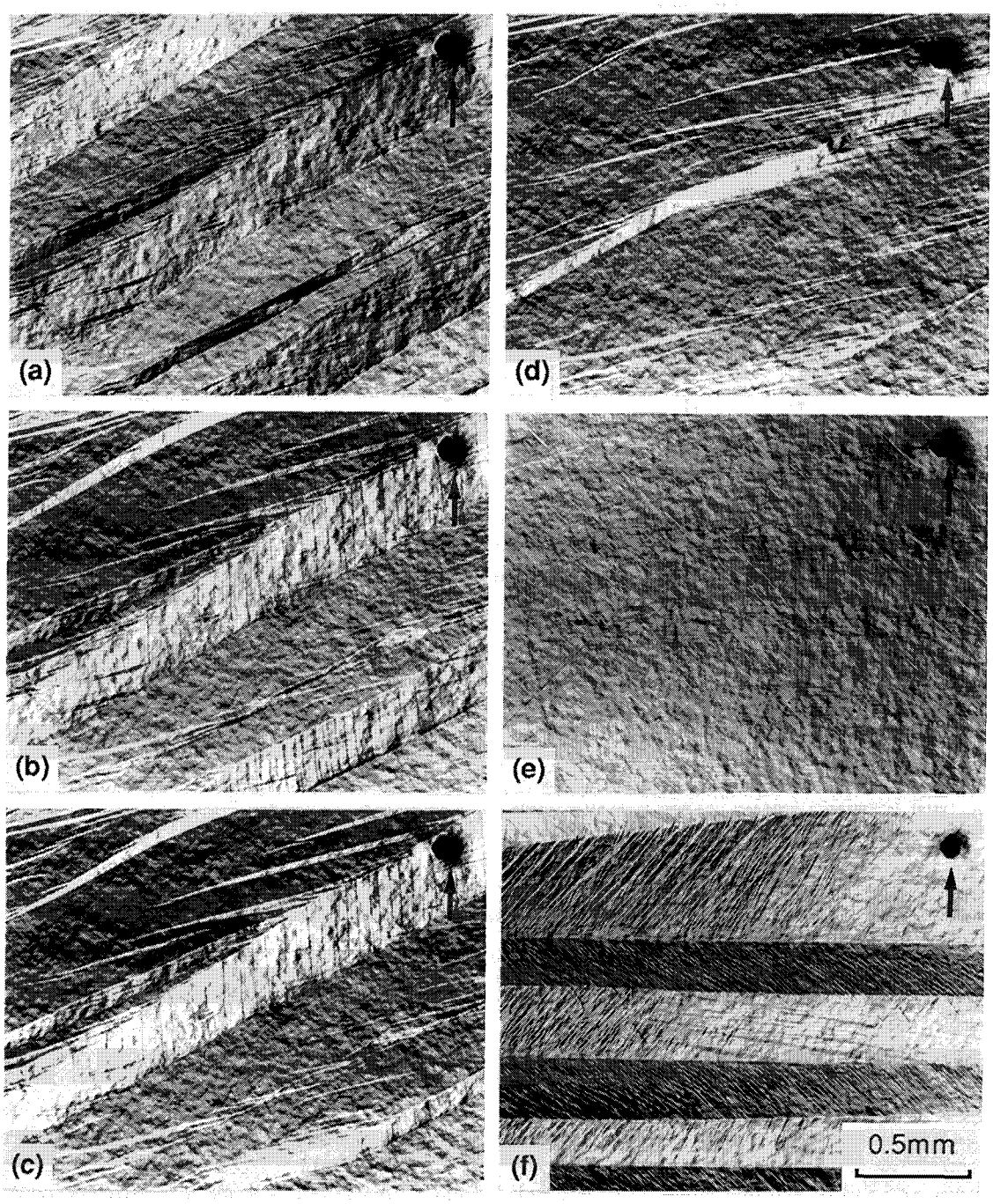

Fig. 2 Optical micrographs showing the change of surface reliefs of a Cu-13.8Al-4.0Ni alloy single crystal. (a) Before tensile test. (b)-(e) Upon tensile test represented in Fig. 1. (f) After the first thermal cycle shown in Fig. 3(b).

ite morphology[15]. The parallel thick bands represent two γ_1' martensite variants with their internal twins inside. Although only two variants are seen in this figure, many more variants were present in the surrounding area. With increasing strain, the morphology changes from (a) to (e), (e) being a γ_1' single crystal martensite. Thus, we confirmed that the first stage in Fig. 1 corresponds to the reorientation of the γ_1' martensite variants into a single crystal martensite. Figure 3(a) shows the electrical resistance change during cooling and heating without deformation. Although there are some noises due to exothermic or endothermic reaction and some vibration during the transformation, M_s and A_s are clear. Figure 3(b) shows the resistance change during heating and cooling after deformation in the martensitic state. We observe clearly that A_s(362 K) is raised to A_s^d(393 K) by the deformation. However, M_s upon cooling is the same as that in Fig. 3(a). If the heating→cooling cycle is repeated once again, Fig. 3(c) is obtained. We clearly observe that A_s returns to the original one in Fig. 3(a). That is, the effect of the A_s increase by pre-deformation is erased from the second heating→cooling cycle.

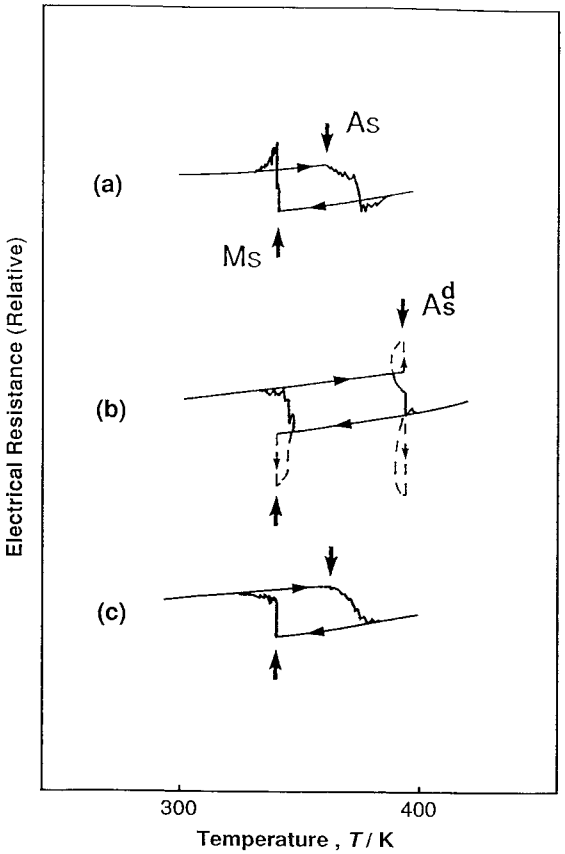

Fig. 3 Electrical resistance vs. temperature curves of a Cu-13.8Al-4.0Ni single crystal. (a) Before tensile test. (b) First cycle after tensile test. (c) After the cycle in (b).

The above behavior is very similar to that observed in a Ti-Ni-Nb alloy[2], and both have common in the characteristics.

The above effect of pre-deformation on the subsequent transformation temperatures may be interpreted in the following way, by focusing attention on the stored elastic strain energy upon the forward transformation. In the as-transformed condition, many variants are present, and the elastic strain energy is stored. However, by the pre-deformation the elastic energy is released from the surface, and at the end of the first stage (Fig. 2(e)), all elastic energy is released. Thus, A_s increases to the characteristic value of the material itself, consistent with Fig. 3(b). Upon cooling after the first reverse transformation, the self-accommodated martensite morphology appears again, as shown in Fig. 2(f). Therefore, A_s goes back to the original one in the next heating cycle (cf. Fig. 3(a) and (c)). Thus, we could explain all the characteristics of the effect of pre-deformation on the transformation temperatures by the above mechanism.

2. Increase of the A_s temperature in Ti-Ni polycrystals

We now discuss the results for Ti-Ni polycrystals. Figure 4 is the tensile behavior of $Ti_{49.5}Ni_{50.5}$ alloy at room temperature. The S-S curve of a Ti-Ni alloy can be divided to three stages[16]-[18], which are represented by I, II, and III in Fig. 4. Because the tensile test temperature (298 K) was slightly above M_s(289 K), the strain in the first stage is due to the stress-induced martensitic transformation. In the second stage, slip deformation of martensite takes place besides the stress-induced transformation of the residual parent. In the third stage, nearly all of the deformation is due to slip, as is analyzed in Fig. 5. Figure 5 shows the recovery characteristics of the specimens deformed to various strains, which were analyzed by the same method in Ref. (18). Here ε_u is the strain after unloading, ε_r the recovery strain caused by the shape memory effect, ε_p the permanent strain and $\varepsilon_u=\varepsilon_r+\varepsilon_p$. The first stage of this alloy is up to 7% total strain (Fig. 4). The strain recovers completely in the first stage, no permanent strain remaining. In the second stage, permanent strain ε_p increases with increasing total strain, and recovery strain ε_r is nearly constant. When the specimen is deformed up to the third stage, ε_p rises linearly with total strain, while ε_r decreases slowly.

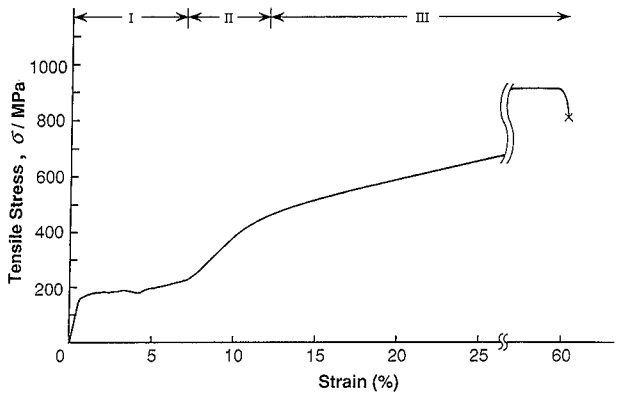

Fig. 4 Stress-strain curve of a $Ti_{49.5}Ni_{50.5}$ alloy polycrystal at room temperature.

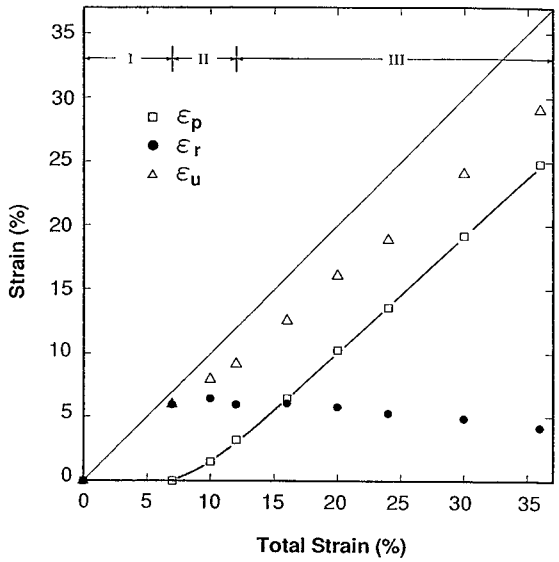

Fig. 5 Variation of ε_p, ε_r and ε_u as a function of total strain ε_t for a $Ti_{49.5}Ni_{50.5}$ polycrystal.

The transformation characteristics of specimens

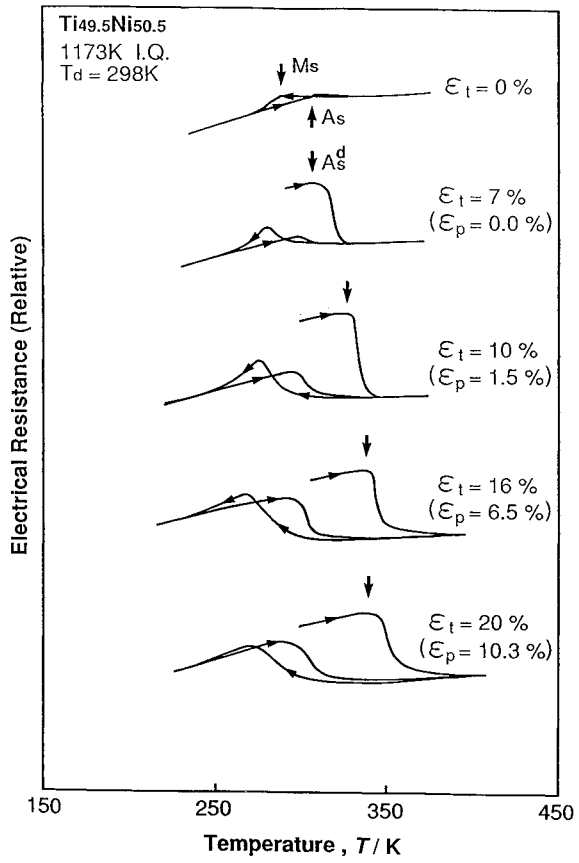

Fig. 6 Effect of deformation on the electrical resistance vs. temperature curve for $Ti_{49.5}Ni_{50.5}$ alloy solution-treated at 1173 K.

deformed to every stage were examined by measuring electrical resistance, and the results are shown in Fig. 6. For every specimen, the resistance measurement was made with heating→cooling→heating cycle, after deformed to the total strain (ε_t) shown in the figure. In the deformed specimens, the resistance continues to increase upon the first heating, then begins to decrease at A_s^d due to the contraction of specimens with reverse transformation[4]. That is, the reverse transformation start temperature A_s changes to a higher temperature A_s^d. When the specimen is deformed to 10% total strain, it shows the maximum recovery strain (Fig. 5), and correspondingly the decrease of the resistance with shape recovery is also maximum. In Fig. 6, it can be found that A_s^d increases with increasing total strain.

Here, some explanations will be necessary, for the change of the electrical resistance vs. temperature (abbreviated below as R-T) curves in the subsequent cooling→heating cycle. Upon cooling after the first reverse transformation, although the resistance decreases immediately at M_s for the undeformed specimen (ε_t=0%), the resistance goes up before the decrease for deformed specimens, leading to a small hump in the R-T curves. Two reasons may be thought for the hump. One is the R-phase transition[19)-23)], and the other is the two-way shape memory effect[24]. As is well known, the resistance sharply increases with the R-phase transition. The two-way shape memory effect leads to an expansion along the tensile direction, causing the increase of resistance. In Fig. 6, the resistance increases almost linearly in the martensitic state upon the second heating, and begins to decrease at a certain temperature, A_s. The decrease is believed to be due to the contraction of the specimen with the reverse transformation, which corresponds to the expansion in the previous cooling cycle. In the specimen deformed 20%ε_t, the resistance sharply increases first and then decreases with cooling as mentioned above. The slope of the R-T curve in the decreasing stage is very similar to the slope of the curve on heating in the martensitic state, and the decrement of resistance with the reverse transformation on the second heating is nearly equal to the increment on the previous cooling. Thus, we conclude that almost all the increment of resistance on cooling is due to the two-way shape memory effect, while the effect of the R-phase transition is little. Comparing the R-T curves in Fig. 6, the effect of the R-phase transition becomes little with increasing total strain.

We now come back to the essential problem of the effect of pre-deformation on the subsequent transformation temperatures. As is clearly seen in Fig. 6, A_s increases to A_s^d by pre-deformation, but the temperature returns nearly to the original one (for ε_t=0) in the subsequent second heating cycle, although A_s in the second cycle is slightly lower than the original one. That is, the effect of pre-deformation vanishes after the first reverse transformation. This characteristic is the same as that in Ti-Ni-Nb alloys and the Cu-Al-Ni single crystal. The increments of A_s (difference between A_s^d and A_s before deformation) obtained from the above results are shown in Fig. 7. The first stage (up to 7%ε_t) of the S-S curve in this alloy represents the stress-induced martensitic transformation. In the stress-induced transformation, the microstructure after the transformation is believed to be essentially similar to that obtained after rearranging variants by tension in the martensitic state, because the martensite variants favorable to tension form and grow under the stress. In such microstructure, interfaces are a few and the elastic strain energy is expected to be relaxed, since the variants favorable to tension grow mostly. Surprisingly, however, A_s of this alloy did not increase by the end of the first stage (ε_t=7%). We can notice from Fig. 5 that no permanent strain is introduced in the first stage. Thus, the effect of pre-deformation apparently looks quite different in the $Ti_{49.5}Ni_{50.5}$ polycrystal and the Cu-Al-Ni single crystal. However, when the specimen is elongated to the second stage, where the permanent strain is introduced, A_s begins to increase. When it is elongated to the third stage, the increment of A_s tends to become a constant. The interpretation of the above results will be made in Section IV, and before doing it, we will introduce the results for the $Ti_{50}Ni_{50}$ alloy.

The essential difference between $Ti_{50}Ni_{50}$ and $Ti_{49.5}Ni_{50.5}$ alloys lies in that slip is more easily introduced in the former[25]. This alloy shows a similar tensile behavior to $Ti_{49.5}Ni_{50.5}$ alloy at room temperature (Fig. 8). Because the transformation temperatures M_s, M_f, A_s and A_f were

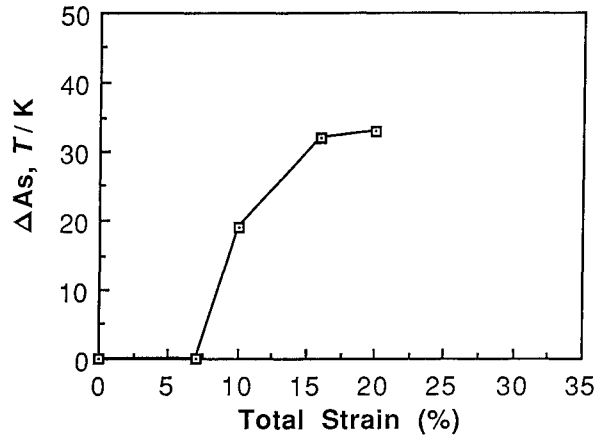

Fig. 7 The increase of A_s as a function of total strain for a $Ti_{49.5}Ni_{50.5}$ polycrystal.

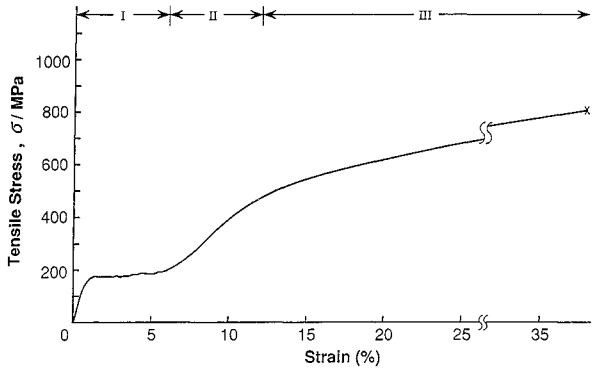

Fig. 8 Stress-strain curve of a $Ti_{50}Ni_{50}$ alloy polycrystal at room temperature.

341, 321, 354 and 368 K respectively, the specimen is in the martensitic state at room temperature and the first stage (up to 6%ε_t) of the S-S curve represents the rearrangement of martensite variants. Figure 9 shows the recovery characteristics of the specimens deformed to various strains. In the first stage, the slip deformation occurs besides rearrangement of variants and thus the permanent strain is introduced, since the yield stress of $Ti_{50}Ni_{50}$ alloy is much lower than that of $Ti_{49.5}Ni_{50.5}$ alloy[25]. With increasing total strain, the permanent strain increases slowly in a low slope in the first stage, and the slope becomes larger gradually in the second stage, finally the permanent strain increases linearly in a high slope in the third stage.

Figure 10 shows the results of the resistance measurements. The *R-T* curves change similar to the $Ti_{49.5}Ni_{50.5}$ alloy with increasing total strain. The increments of A_s are shown in Fig. 11. A_s increases rapidly until the second stage, and the increment tends to saturate in the third stage. The difference from $Ti_{49.5}Ni_{50.5}$ alloy is that A_s rises even in the first stage (6%ε_t), which corresponds to the fact that the permanent strain appears in the first stage. It means that the A_s increase is closely related to the permanent strain. Figure 12 shows the relation between increment of A_s and permanent strain in the two Ti-Ni alloys. It is clear that A_s does not increase without permanent strain introduced in both alloys. The above results clearly indicate that there is a close correlation between A_s increase and the permanent strain in polycrystals.

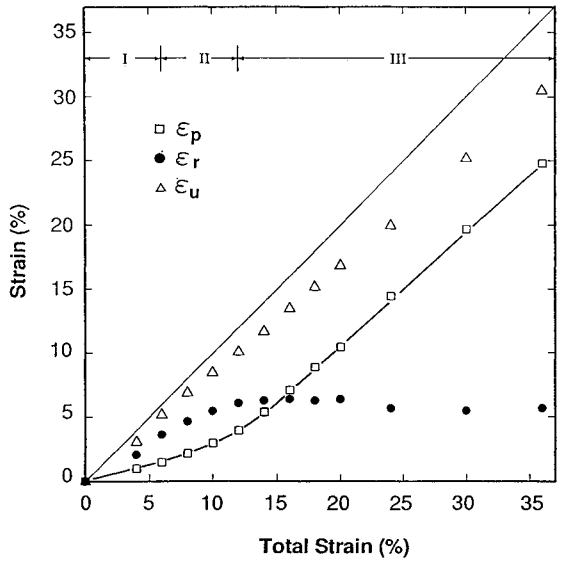

Fig. 9 Variation of ε_p, ε_r and ε_u as a function of total strain ε_t for a $Ti_{50}Ni_{50}$ polycrystal.

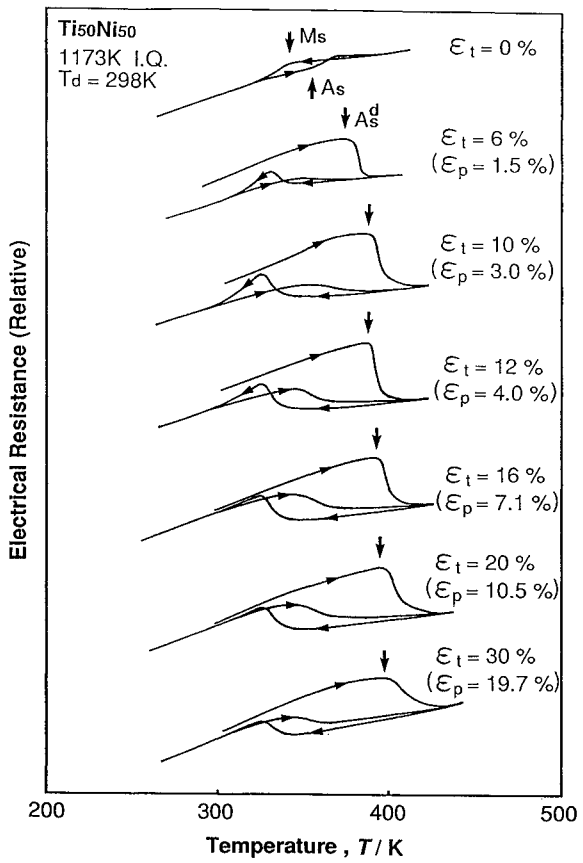

Fig. 10 Effect of deformation on the electrical resistance vs. temperature curve for $Ti_{50}Ni_{50}$ alloy solution-treated at 1173 K.

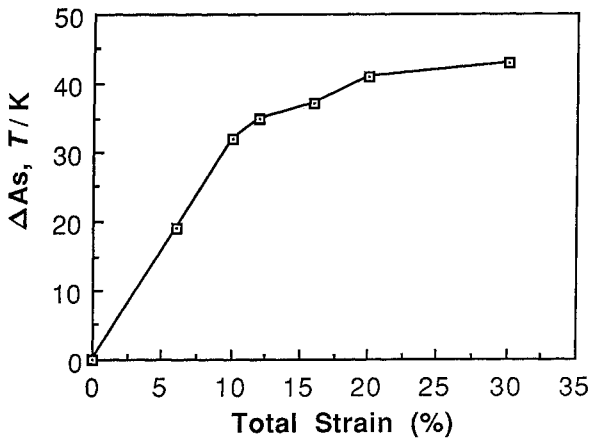

Fig. 11 The increase of A_s as a function of total strain for a $Ti_{50}Ni_{50}$ polycrystal.

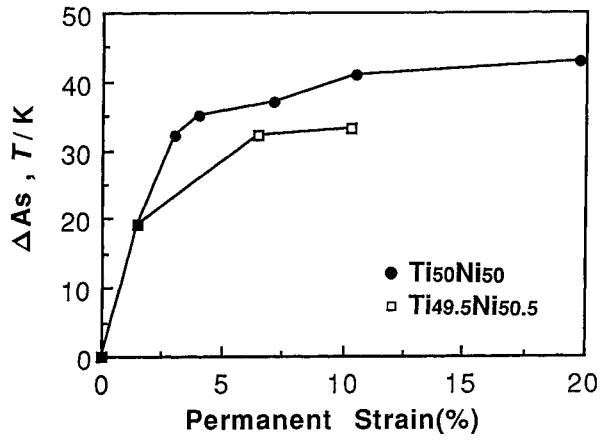

Fig. 12 The increase of A_s as a function of permanent strain for $Ti_{50}Ni_{50}$ and $Ti_{49.5}Ni_{50.5}$ polycrystals.

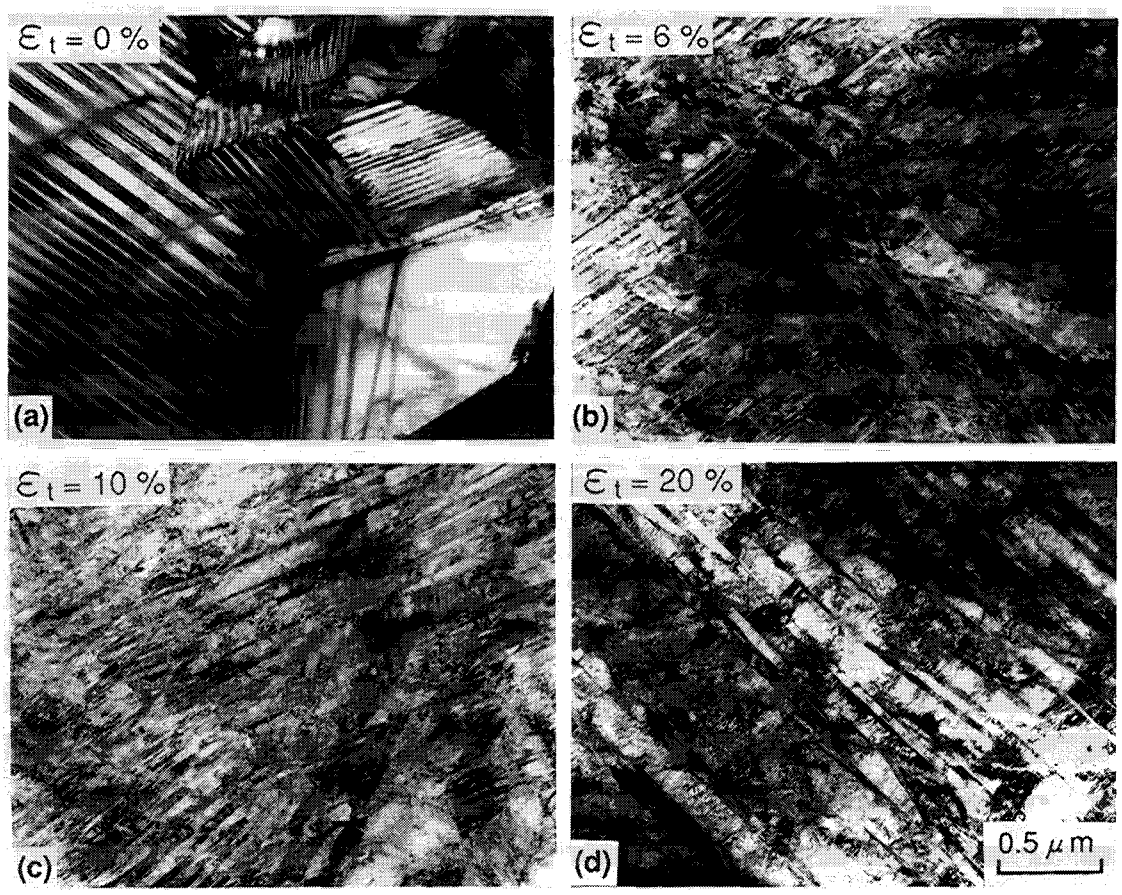

Fig. 13 TEM micrographs of $Ti_{50}Ni_{50}$ alloy deformed. (a) ε_t=0%, (b) ε_t=6%, (c) ε_t=10% and (d) ε_t=20%.

Figure 13 shows TEM micrographs of the $Ti_{50}Ni_{50}$ alloy, in which (a) is the micrograph before deformation and (b)-(d) those after deformed to the first, the second and the third stage respectively. In the undeformed condition (Fig. 13(a)), martensite variants with various orientations formed thermally. Stripes appearing in every variant are internal twins. The difference of the stripe directions shows the difference of orientations between variants. From these observations, a tendency is observed such that various martensites tend to rearrange to a single orientation by deformation even in polycrystals. These specimens were also observed after heating to the parent phase at 523 K, as shown in Fig. 14. Compared with the undeformed specimen, dark contrasts are observed in deformed specimens. Figure 15(a) is a magnified micrograph of Fig. 14(d), and Fig. 15(b) is the

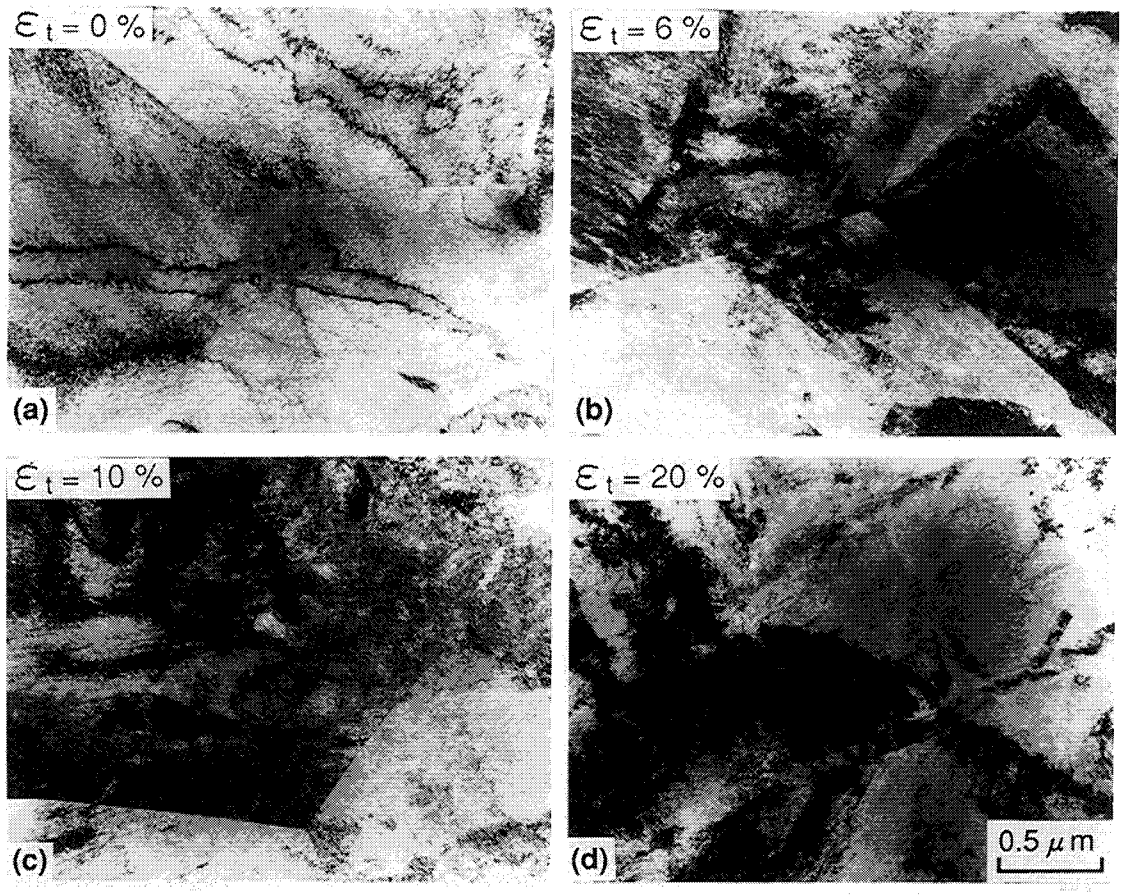

Fig. 14 TEM micrographs of the samples shown in Fig. 13 taken in the parent phase (at 523 K).

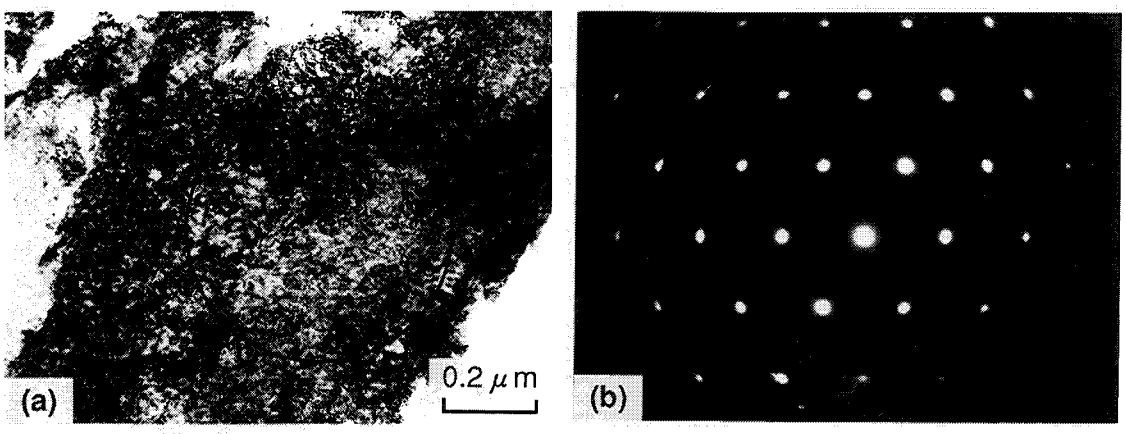

Fig. 15 (a) High magnification TEM micrograph of the sample shown in Fig. 14(d) taken at 523 K. (b) Electron diffraction pattern taken from the encircled region in (a).

electron diffraction pattern taken from the encircled region in (a). The dark contrast appears to be a cluster of small dislocation loops. The diffraction pattern agrees with [111] zone of the CsCl(B2) structure, from which the specimen is confirmed to be in the parent state at the observed temperature. Figure 16 shows the internal structures of the deformed specimens which were subjected to heating to the parent phase, subsequently cooled into the martensitic state again. We observe the self-accommodating morphology of various martensite variants. This means that the elastic strain energy is restored again after the first reverse transformation.

IV. Discussion

We now discuss the mechanism for the A_s increase by pre-deformation, by focusing attention on stored elastic strain energy in thermoelastic alloys. The case for the

Cu-Al-Ni single crystal is straightforward, as discussed in Section III. 1. When the alloy is transformed into the martensite, the elastic energy is stored in the self-accommodating morphology. Thus, A_s is lower than the characteristic value of the material itself. However, when the alloy single crystal is pre-deformed in the martensitic state, the martensite variants rearrange themselves into a single variant, relieving the strain energy from the surface. Thus, A_s increases to the characteristic value of the material itself, as observed. However, upon cooling after the reverse transformation, many variants reappear again, storing the elastic energy. Therefore, A_s returns to the original value without deformation. Thus, our mechanism was confirmed by the above single crystal experiments.

The cases of polycrystals are not so straightforward, but we will show in the following that the same mechanism apply for the cases as well. Obviously the essential difference between a polycrystal and a single crystal is the presence of grain boundaries. Because of the constraints of grain boundaries, the stored elastic strain energy is not relieved, even though a grain tends to become a single crystal of the martensite. This is most typically shown in the first stage of the S-S curve of the $Ti_{49.5}Ni_{50.5}$ alloy, since no A_s increase was observed in the stage. We believe the strain energy is still stored elastically in this case. Since A_s increase is closely related with the introduction of permanent strain, we can postulate that the stored elastic energy can be relieved only by the introduction of slip upon rearrangement of martensite variants in polycrystals. Then, we can explain all the characteristics of the effect of pre-deformation in polycrystals. Since no slip is introduced in the first stage in the $Ti_{49.5}Ni_{50.5}$ alloy, the A_s increase is observed only after the first stage (Fig. 7), while since slip is introduced even in the first stage in the $Ti_{50}Ni_{50}$ alloy, A_s increases even in the first stage (Fig. 11). Since self-accommodating morphology appears again upon cooling after the first reverse transformation (Fig. 16), the elastic strain energy is restored upon the subsequent forward transformation. Thus, A_s returns to nearly the original value without deformation. The slight decrease of A_s in the second cycle relative to the original value without deformation (Fig. 6 and Fig. 10) is due to the introduction of dislocations (Fig. 15), which stabilizes the parent phase.

The final problem is to analyze the A_s increase by pre-deformation in Ti-Ni-Nb alloys. As seen from Fig. 17, the A_s increase in $Ti_{44}Ni_{47}Nb_9$ alloy is greater than that of the $Ti_{50}Ni_{50}$ alloy. Fig. 18 shows the TEM micrograph and electron diffraction patterns of $Ti_{44}Ni_{47}Nb_9$ alloy deformed 12%ε_t. Many islands of the Nb-rich phase are observed in Fig. 18(a), as confirmed by the corresponding electron diffraction pattern of (b). Figure 18(c) taken from the region marked "B" in matrix confirms

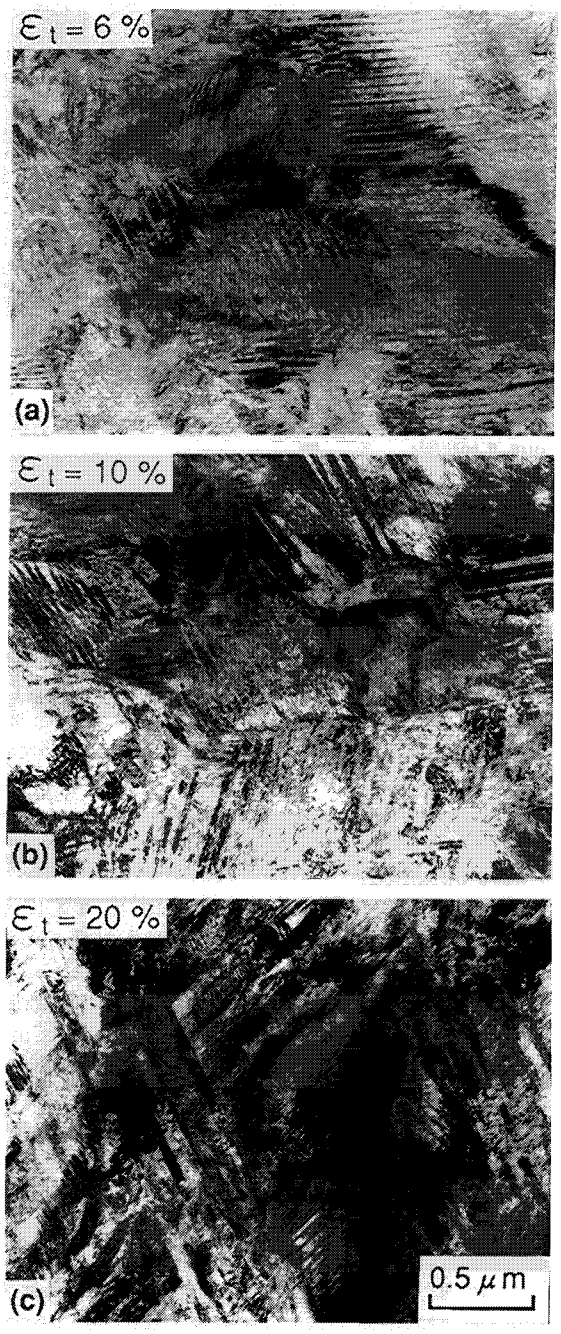

Fig. 16 TEM micrographs of $Ti_{50}Ni_{50}$ alloy after one cycle of heating and cooling after the deformation in the martensitic state.

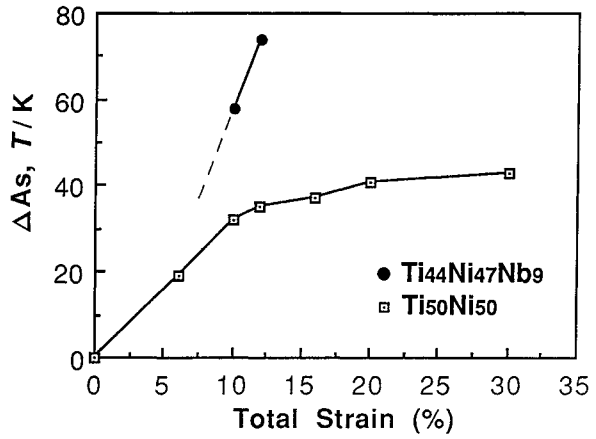

Fig. 17 Comparison of increment of A_s between $Ti_{44}Ni_{47}Nb_9$ alloy and $Ti_{50}Ni_{50}$ alloy.

that the structure of the surrounding area is B2 type structure. Compared with the structure of the undeformed specimen (Fig. 19(a)), many dislocations are observed in the Nb-rich phase of the specimen deformed (Fig. 19(b)). It means that a large amount of permanent strain are introduced in the Nb-rich phase by the pre-deformation. Thus, the large amount of A_s increase in the Ti-Ni-Nb alloy may be due to the plastic deformation of the Nb-rich phase dispersing in the matrix, which effectively relaxes the elastic strain energy. Besides, the effect of the deformed Nb-rich phase resisting the shape recovery of matrix[8] may act additionally.

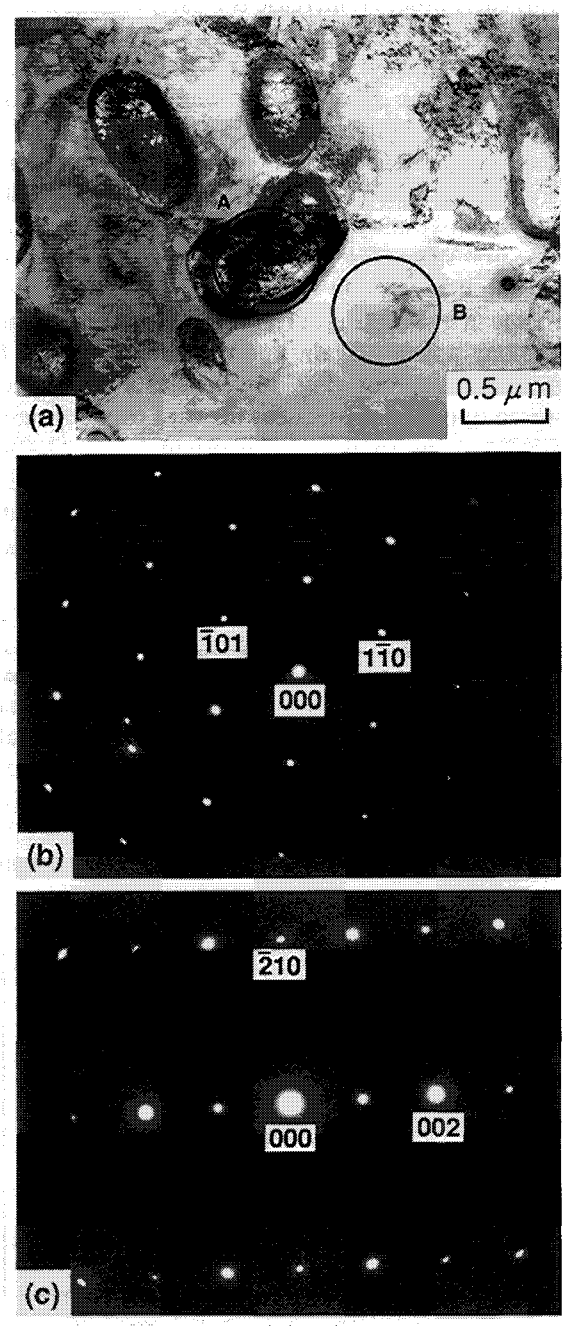

Fig. 18 (a) TEM micrograph of $Ti_{44}Ni_{47}Nb_9$ alloy deformed 12%. (b) Electron diffraction pattern of Nb-rich phase taken from the encircled region **A** in (a). (c) Diffraction pattern of Ti-Ni phase taken from the encircled region **B** in (a).

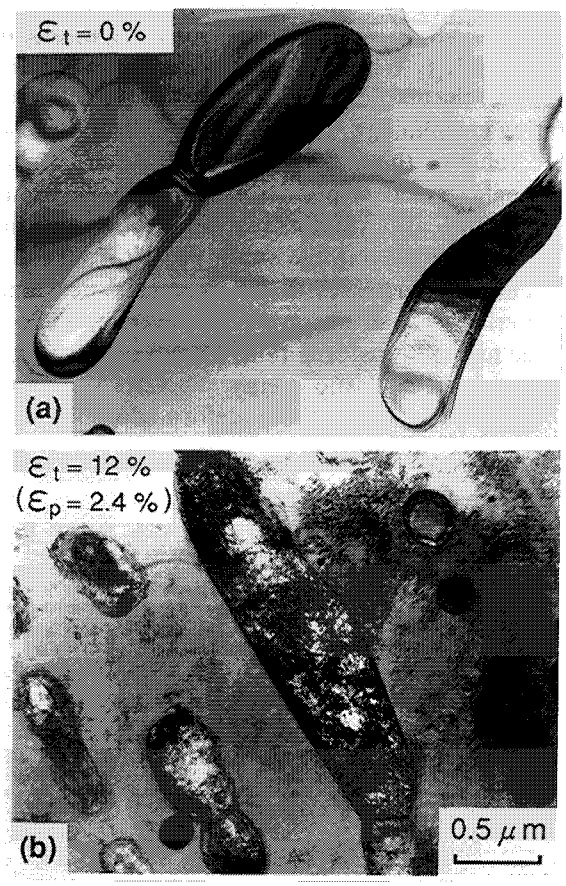

Fig. 19 Comparison of internal structures between undeformed and deformed specimens of $Ti_{44}Ni_{47}Nb_9$ alloy.

V. Conclusions

A mechanism for the A_s increase by pre-deformation in thermoelastic alloys is proposed in this study. That is, the pre-deformation relaxes the stored elastic strain energy in multivariants martensites, and results in the increase of A_s. The mechanism was verified by using a Cu-Al-Ni alloy single crystal and $Ti_{50}Ni_{50}$, $Ti_{49.5}Ni_{50.5}$, $Ti_{44}Ni_{47}Nb_9$ alloy polycrystals, and the following conclusions were obtained.

(1) The A_s increase was confirmed in a Cu-Al-Ni alloy single crystal, after it was deformed in the martensitic state until the specimen became a single variant. This effect is interpreted in the following way. Upon cooling, the elastic strain energy is stored in the self-accommodating morphology of various martensites. Upon rearrangement into a single variant by pre-deformation, the strain energy is released from the surface, thus leading to the increase of A_s. In the second cycle after the first reverse transformation, A_s returns to the original one without deformation, since the self-accommodating morphology is regained.

(2) The A_s increase was also observed in the Ti-Ni alloy polycrystals. It was confirmed that the A_s increase in polycrystals is closely related with the permanent strain, i.e. A_s never increased without introducing slip in

polycrystals. By postulating that slip relaxes the stored elastic strain energy in the martensite, it is possible to explain all the characteristics of the effect of pre-deformation on the transformation temperatures.

(3) It was clarified that the A_s increase by pre-deformation is a common characteristic in thermoelastic alloys.

(4) The increment of A_s in Ti-Ni-Nb alloys was greater than that in Ti-Ni alloys. The reason is interpreted such that the plastic deformation of the Nb-rich phase relaxes more effectively the stored elastic strain energy. The resistance of the deformed Nb-rich phase against the shape recovery of matrix during the reverse transformation may act as the second source for the A_s increase.

Note added in proof: There was a report on the effect of cold rolling on the martensitic transformation in a coarse grained Cu-Al-Ni alloy by Martynov *et al.*[26]. They observed the increase of reverse transformation temperatures by cold rolling and suggested the contribution of elastic energy as a possible cause in addition to the lattice defects. However, ther is no clear proof showing the effect of elastic energy, and the description is extremely brief both in experiments and discussions. The authors thank Dr. Martynov for drawing our attention to their paper.

Acknowledgment

The authors express their hearty thanks to Dr. K. Furuya at National Research Institute for Metals, for the use of a dimpling instrument to make TEM samples and the use of a heating holder for TEM observation at high temperature.

REFERENCES

(1) K. N. Melton, J. Simpson and T. W. Duerig: *Proc. Int. Conf. on Martensitic Transformations (ICOMAT-86)*, Japan Inst. Metals, (1986), p. 1053.
(2) K. N. Melton, J. L. Proft and T. W. Duerig: *Proc. MRS Int. Mtg. on Adv. Mats.*, Tokyo, **9** (1989), p. 165.
(3) M. Piao, S. Miyazaki, K. Otsuka and N. Nishida: Mater. Trans., JIM, **33** (1992), 337.
(4) M. Piao, S. Miyazaki and K. Otsuka: Mater. Trans., JIM, **33** (1992), 346.
(5) L. C. Zhao, T. W. Duerig and C. M. Wayman: *Proc. MRS Int. Mtg. on Adv. Mats.*, Tokyo, **9** (1989), p. 171.
(6) L. C. Zhao, T. W. Duerig, S. Justi, K. N. Melton, J. L. Proft, W. Yu and C. M. Wayman: Scripta Met., **24** (1990), 221.
(7) C. S. Zhang, L. C. Zhao, T. W. Duerig and C. M. Wayman: Scripta Met., **24** (1990), 1807.
(8) T. W. Duerig and K. N. Melton: *The Martensitic Transformation in Science and Technology*, (1989), p. 191.
(9) T. W. Duerig, K. N. Melton and J. L. Proft: *Engineering Aspects of Shape Memory Alloys*, (1990), p. 130.
(10) W. J. Buehler and W. B. Cross: Wire Journal, June (1969).
(11) H. G. Tong and C. M. Wayman: Acta Met., **22** (1974), 887.
(12) G. B. Olson and M. Cohen: Scripta Met., **9** (1975), 1247.
(13) R. J. Salzbrenner and M. Cohen: Acta Met., **27** (1979), 739.
(14) H. Sakamoto and K. Shimizu: ISIJ International, **29** (1989), 395.
(15) K. Otsuka and K. Shimizu: Trans. JIM, **15** (1974), 103.
(16) A. G. Rozner and R. J. Wasilewski: J. Inst. Metals, **94** (1966), 169.
(17) W. B. Coss, A. H. Kariotis and F. J. Stimler: NASA CR-1433, (1969).
(18) S. Miyazaki, K. Otsuka and Y. Suzuki: Scripta Met., **15** (1981), 287.
(19) H. G. Ling and R. Kaplow: Met. Trans. A, **12A** (1981), 2101.
(20) C. M. Hwang, M. Meichle, M. B. Salamon and C. M. Wayman: Phil. Mag., **47** (1983), 9.
(21) S. Miyazaki and K. Otsuka: Met. Trans. A, **17A** (1986), 53.
(22) M. Matsumoto and T. Honma: *Proc. Ist JIM Int. Symp. on New Aspects of Martensitic Transformation*, Supplement to Trans. JIM, **17** (1976), p. 199.
(23) M. Nishida and T. Honma: J. de Phys., **43** (1982), c-225.
(24) A. Nagasawa, K. Enami, Y. Ishino, Y. Abe, S. Nenno: Scripta Met., **8** (1974), 1055.
(25) S. Miyazaki, Y. Kohiyama and K. Otsuka: *Proc. Int. Symp. on Intermetallic Compounds (JIMIS-6)*, Sendai, (1991), p. 269.
(26) V. V. Martynov, P. V. Titov, L. G. Khandros: Metallophysika, No. 48, *Naukova Dumka*, Kiev, (1973), 43, (in Russian).